EXPERIMENTAL INVESTIGATION AND MODELLING OF THE VISCOSITY OF OXIDE SLAG SYSTEMS

Michael MÜLLER[1], Sören SEEBOLD[1], Guixuan WU[1], Elena YAZHENSKIKH[1], Tatjana JANTZEN[2], Klaus HACK[2]

[1] Forschungszentrum Jülich GmbH, Institute of Energy and Climate Research, IEK-2, 52428 Jülich, Germany

[2] GTT-Technologies, 52134 Herzogenrath, Germany

mic.mueller@fz-juelich.de

Introduction

Numerous technical applications in the energy and metallurgical industries demand a fundamental knowledge of the flow of slags. As an example, in entrained flow gasification of solid fuels the molten oxide slag has to be continuously removed from the gasifier. A viscosity of the slag below 25 Pa*s is desirable[1].

Many experimental investigations on the influence of composition and temperature on the viscosity of slags have been conducted as summarised for example by Allibert or Vargas[2, 3]. The dependence on temperature for fluids in general is described by the Arrhenius-law which can be expressed as:

$$\eta = A*\exp(E/(R*T)), \quad (1)$$

where η is the dynamic viscosity, T is the absolute temperature, E is the activation energy for viscous flow, R is the gas constant, and A is a composition-dependent constant. The decrease of temperature results in an exponential increase of viscosity according to the Arrhenius law. For most technical applications, the influence of pressure is negligible due to the low effect of pressure on fluids. Silicate melts behave in this regard similar[4]. The influence of composition on the viscosity is more complicated. Molten slags are treated as a mixture of oxides. Based on the network theory postulated by Zachariasen[5], these oxides are categorised regarding their role in the network as network former (*e.g.* SiO_2), network modifier (*e.g.* CaO, MgO, FeO, Na_2O, K_2O) or amphoteric (*e.g.* Al_2O_3, Fe_2O_3). A network former can increase the viscosity, whereas a network modifier usually decreases the viscosity by breaking the bonds between silicon ions and oxygen ions of the tetrahedral structure. Depending on the composition, an amphoteric can behave as either a network former or a network modifier. Different empirical and semi-empirical models such as the Urbain model[6] have been proposed to describe the viscosity of a slag. These models are usually limited to a specific composition range.

Below the melting temperature some slags show a steep increase of viscosity deviating from the Arrhenius law. At this so-called temperature of critical viscosity (T_{CV}) the fully

molten slag transforms into a partially crystalline slag[7, 8]. The crystalline phases increase the viscosity and also influence the flow behaviour, therefore non-Newtonian flow may occur[7, 9].

During recent years IEK-2 of Forschungszentrum Jülich and GTT were given the opportunity to cooperate in the framework of several projects on the development of a novel thermochemical database and a new viscosity model. In addition, own experimental work could be carried out to investigate the behaviour of fuel slags and related oxide systems.

Experimental

High-temperature viscometer

A viscometer RC1 (Rheotec, Dresden, Germany) is used in combination with a furnace developed in-house as schematically shown in Figure 1. In the furnace, there is a dense alumina tube surrounded by three $MoSi_2$ heating elements, enabling measurements up to 1700°C. The slag containing crucible is placed on the top of a second alumina tube within a zone of constant temperature. The temperature of the specimen is controlled by a thermocouple Type S, placed directly below the crucible, enabling a precise temperature measurement as close to the slag as possible. The viscometer is attached by a universal joint to a magnetic coupling, which encloses the heating room. Crucible and spindle have a diameter of 26 mm and 14 mm, respectively. Both consist of molybdenum, because of the high melting point and the good resistance regarding oxide melts. To prevent them from oxidation measurements are conducted in Ar/4% H_2. The length of the spindle is about 250 mm. The short length offers a stable concentrically rotation of the spindle during the measurement.

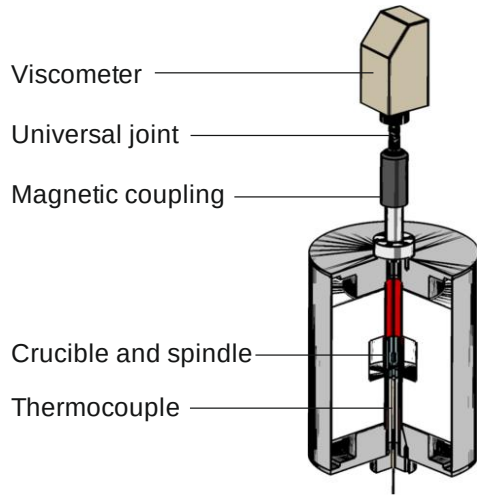

Figure 1: Schematic drawing of the high temperature viscometer

The approach is based on the wide-gap concentric cylinder method. The ratio of inner radius to the outer radius is a crucial criterion for the flow pattern between the wall of

the crucible and the rotating spindle during the viscosity measurements[10]. Due to the ratio (r_o/r_i = 1.86) employed the system is non-ideal and has to be calibrated. Calibration was performed using the standard glass G1 (PTB, Germany). The calibration was validated by measuring two additional standard glasses, DGG1 (HVG, Germany) and G3 (PTB, Germany). The maximum deviation between the experimentally determined viscosities and the reference values was about 10%.

Measurement procedure

Stepwise and isothermal measurements are used to characterise the evolution of viscosity. During stepwise measurements, the slag is cooled stepwise to a lower temperature, starting from a temperature above the fluid temperature of the ash determined by an ash fusion test (AFT). To ensure homogeneity the slag is stirred by the spindle during cooling and at constant temperature. After achieving thermal equilibrium, the measurement is started. First, the maximum shear-rate is determined. Therefore, the rotational speed is increased until the maximum torque is reached. This is required to enable a measurement over a wide range of shear-rates to increase the accuracy of the measurement. Then the shear-rate is increased stepwise until reaching the maximum. In these measurements T_{CV} and the onset of non-Newtonian flow behaviour indicate the crystallisation.

The second procedure is a method to investigate the evolution of flow during crystallisation under isothermal conditions. The measurement consists of three parts. In the first step, the slag is melted by heating above the fluid temperature. After waiting for at least 30 min the sample is cooled down to the targeted experimental temperature with a constant cooling rate of 10 K/min. During this time the slag is already stirred to ensure homogenisation. Then, the isothermal measurement is conducted. The temperature is held for a certain duration, depending on the crystallisation behaviour of the slag. A low shear rate is chosen for the isothermal measurement, as the stirring influences the crystallisation behaviour[11]. At the end of the measurement the flow behaviour is investigated by raising the speed of the spindle until reaching the maximum torque. The isothermal procedure is repeated for different temperatures to get a detailed view on effects of crystallisation on the flow of coal ash slags.

Experimental results

As an example, results of measurements for a German hard coal ash (ST-D-2) are presented[12]. Its composition is given in Table 1. Figure 2 shows the results of the stepwise measurements. For comparison, also the results of a German lignite coal ash (HKT) are presented. The plotted viscosity is the average of 20 shear dependent measurements at each temperature step. Consequently, an apparent viscosity is described at temperatures below T_{CV}. Both slags show ideal behaviour above 1250°C, which can be described by the Arrhenius-law. However, for temperatures below

1250°C HKT shows a non-ideal abrupt increase of viscosity due to crystallisation. In contrast, there is no clear indication of crystallisation for ST-D-2.

Table 1: Composition in wt% of the ashes from the coals HKT and ST-D-2 ashed at 815°C, analysed by ICP-OES, and normalised according to the highest oxidation state

	SiO_2	Al_2O_3	CaO	Fe_2O_3	MgO	K_2O	Na_2O	TiO_2
ST-D-2	47.1	23.3	8.2	11.2	4.6	2.5	1.6	<1
HKT	52.4	20.0	14.2	2.5	5.9	<1	2.7	1.3

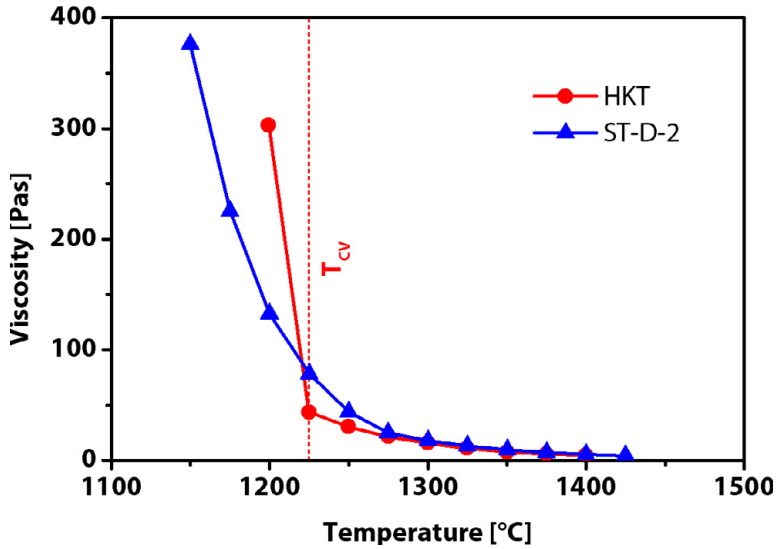

Figure 2: Apparent viscosity of the slags HKT and ST-D-2 plotted versus temperature

Figure 3 shows the results of the isothermal measurements on STD-2, which offer the possibility to investigate the evolution of viscosity as function of time with temperature step-wise held constant. The results indicate crystallisation during the isothermal measurement. The process of crystallisation induces a time dependence of the apparent viscosity at temperature below 1200°C. The effect of crystallisation is significant and strongly increases the apparent viscosity. The results illustrate the importance of temperature as well as time in crystallisation processes.

The evolution of viscosity in experiments with targeted constant temperatures below the melting point can be divided into four parts. The first part is the thermal relaxation, which is not shown in Figure 3. The cooling of the sample to the targeted temperature causes a strong rise of viscosity. The viscosity increases according to Arrhenius exponentially with linear temperature decrease. The second part is the incubation. This lag time is the sum of two characteristic times, the time needed for the formation of a sufficient number of critical nuclei and the time required arriving at a constant rate of crystal growth. In the range of lag time the apparent viscosity is invariant. The third part is the crystallisation. The beginning of crystallisation is observed due to the increase of viscosity. The nucleation rate and the rate of crystal growth influence the development of crystallisation rate and therefore the evolution of viscosity. The fourth

and last part is the rheological equilibrium. The viscosity is time invariant in this part. The process of crystallisation finishes, the liquid slag is in equilibrium with the solid precipitates. It cannot be excluded that crystallisation of another phase will begin. The time durations for the measurement are not completely sufficient to describe the thermodynamic equilibrium, so the term rheological equilibrium is used.

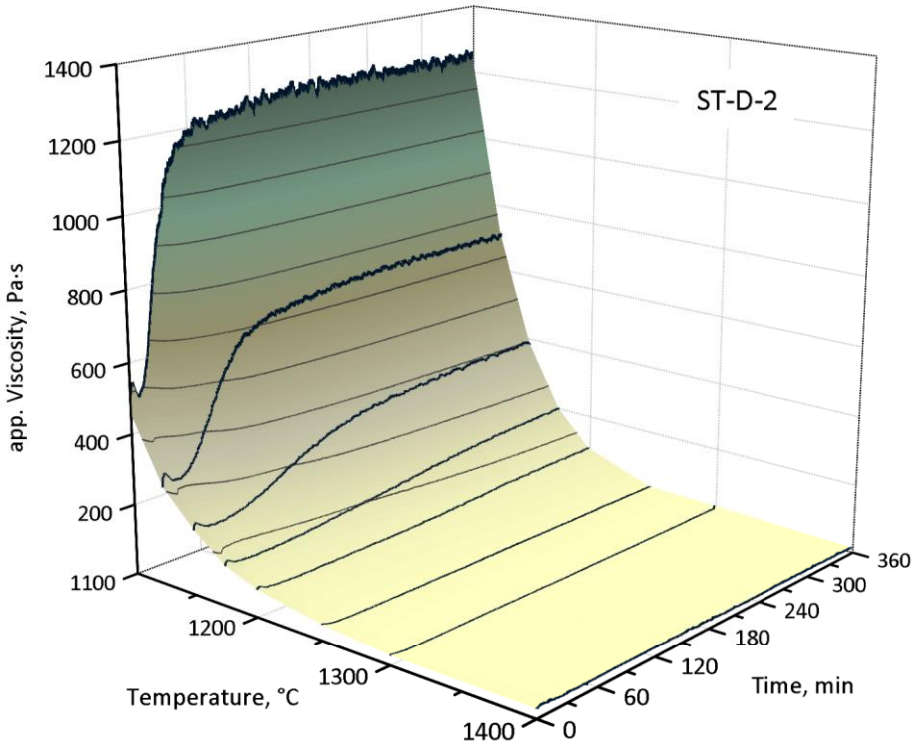

Figure 3: Results of the isothermal viscosity measurements for ST-D-2

Viscosity modelling

As the experimental results reveal, a model for an accurate description of the flow of a slag in a wide range above and below its melting temperature needs to consider the viscosity of the melt itself depending on chemical composition and temperature as well as the physical and chemical influence of the precipitating crystals. Therefore, a new structure based model, which we call the modified Arrhenius model, has been developed to describe the viscosity behaviour of fully molten slags[13,14]. Since the structure of the slag is derived from thermodynamic calculations using our new database, a short overview of our thermochemical assessment work will be given first. Finally, a concept to extend the model from fully molten slags to partially crystallised slags is introduced.

Thermodynamic modelling of oxide systems

This chapter is supposed to give an overview of the models used and the present state of the database. Detailed reports on several of the assessments of subsystems can be found in respective publications[15-21].

The different phases in the respective binary, ternary and higher-order subsystems have been treated with Gibbs energy models which reflect their respective peculiarities. The simplest case for modelling are the solid stoichiometric compounds, *i.e.* solids with a given chemical formula such as Al_2O_3, since these only have a temperature dependent G°(T)-function, usually of the type:

$$G° = A + B*T + C*T*\ln(T) + D*T^2 + E*T^3 + F/T \quad (2)$$

However, often such stoichiometric compounds are actually end members of solids solutions, in the case of Al_2O_3 it is the corundum phase with the component oxides Al_2O_3, Fe_2O_3 and Cr_2O_3. One could argue that these three represent the end members of a substitutional solution. However, even this phase is best treated by a multi-sublattice approach, here with one sublattice for the three trivalent cations and one for the divalent oxygen anion: $(Al^{3+},Fe^{3+},Cr^{3+})_2(O^{2-})_3$. A more striking case is the spinel solid solution with the phase formula $(Al^{3+},Fe^{2+},Fe^{3+},Mg^{2+},Cr^{2+},Cr^{3+})_1(Al^{3+},Ca^{2+},Fe^{2+},Fe^{3+},Mg^{2+},Cr^{3+},Va°)_2(Fe^{2+},Mg^{2+},Cr^{2+},Va°)(O^{2-})_4$. In this case, there are three sublattices on which mixing between different cations and even vacancies Va takes place while the oxygen anion sublattice has fixed occupancy. The general Gibbs energy equation for multi-sublattice phases was given by Sundman and Agren[22] and reads:

$$G_m = \sum_{I_0} P_{I_0}(Y)\,{}^0G_{I_0} + T \cdot R \sum_{s=1}^{n} a_s \sum_{i=1}^{n_s} y_i^{(s)} \ln(y_i^{(s)}) + \sum_{I_1} P_{I_1}(Y) L_{I_1} + \sum_{I_2} P_{I_2}(Y) L_{I_2} + \ldots \quad (3)$$

In this, I_0 is a constituent array of zeroth order specifying one constituent in each sublattice, *i.e.* an end member compound of the phase, $P_{I_0}(Y)$ is the product of the constituent fractions specified by I_0, $°G_{I_0}$ is the compound-energy parameter representing the Gibbs energy of formation of the compound I_0, a_s is the number of sites on each sublattice, and $y_i^{(s)}$ is used to denote the constituent fraction of I on sublattice s. For details see for example Lukas, Fries and Sundman[23].

The liquid phase, often called slag in the context of oxide databases, which exhibits on the one hand short-range ordering, *i.e.* strong attractive interactions, and on the other hand ranges of immiscibility, *i.e.* strong repulsive interactions, was modelled using the non-ideal associate model according to Spear and Besmann[24] described in more detail elsewhere[15]. The Gibbs energy of formation of the associates essentially represents the strong attractive interactions while the repulsive interactions are treated by the classical Redlich-Kister polynomial.

$$G_m = \sum x_i G_i^0 + R \cdot T \sum x_i \ln x_i + \sum \sum_{i<j} x_i x_j \sum_{\nu=0} L_{ij}^{(\nu)} (x_i - x_j)^\nu \quad (4)$$

In this equation, the summation index i includes both the component oxides and the associate species. The G°- and L-parameters in the above equation are temperature dependent as in Equation (2). It should however be noted that for the L-terms usually only the first two terms are needed.

Up to now, a self-consistent thermodynamic database for the system Al_2O_3-Al_2S_3-CaO-CaF_2-CaS-Cr_2O_3-FeO-Fe_2O_3-FeS-MgO-MgS-MnO-Mn_2O_3-MnS-K_2O-K_2S-Na_2O-Na_2S-P_2O_5-SiO_2-SO_3 has been established which permits the calculation of phase diagrams and thermodynamic properties for any composition and temperature. Using this database, a good agreement in terms of phase diagrams and activities is achieved as shown elsewhere[15-21]. Furthermore, the modified associate species model can give a reliable distribution of associate species, which is consistent with the experimentally determined Q^n species distribution as shown in Figure 4 for the system SiO_2-Na_2O, in which the species Q^2, Q^3 and Q^4 correspond to the associate species Na_2SiO_3, $Na_2Si_2O_5$ and SiO_2, respectively. Thus, the associate species distribution gives a good base to represent the internal structure of the molten slag.

Modelling of the viscosity of oxide melts

As shown in Equation (1), the Arrhenius-like models can effectively calculate the viscosity of a system, which consists of only one species. Equation (1) can be transformed to the logarithmic form:

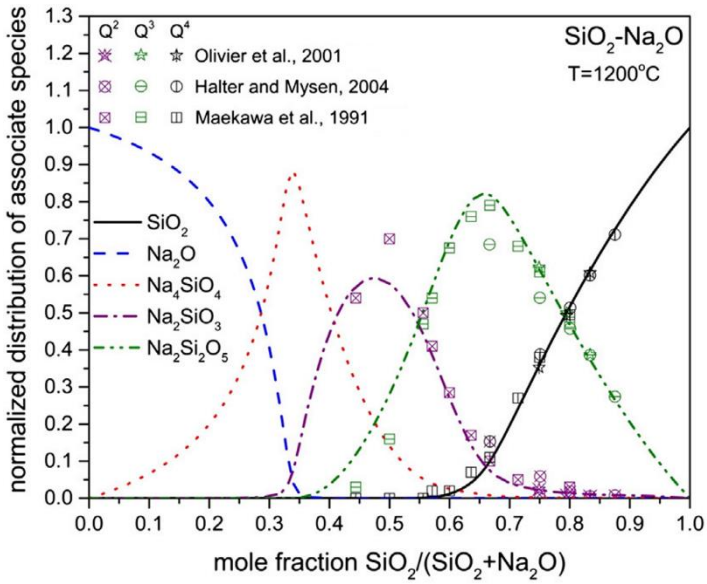

Figure 4: Normalised distribution of associate species for the system SiO_2-Na_2O

$$\ln \eta = A' + 1000 * B/T, \quad (5)$$

where: A' = ln A and B = E/(1000*R). However, calculating the viscosity of a multicomponent melt, which consists of various species, is challenging.

Each associate species used for the thermodynamic description of the melt represents one kind of structural unit as shown before. Therefore, the slag structure can be described with the associate species distribution at some level. However, using this distribution is not sufficient, since the associate species themselves are not sensitive to their own connectivity. In pure silica melt, for example, the structure is described with only one associate species SiO_2, even though the pure silica melt consists of various silica clusters[25], which can be related to the connectivity of the associate species SiO_2. A higher degree of connectivity, which can be reflected by the degree of polymerisation reaction, results in a larger structural unit, and therefore an increased viscosity. The viscosity of the system consisting of various species, therefore, can be described with two parts: an ideal viscosity part and an excess viscosity part. The ideal viscosity part is based on the assumption that every associate species is a discrete structural unit without any polymerisation. The excess viscosity part results from the critical silica polymerisations that have significant contributions to the viscosity. In the SiO_2-based systems, the excess viscosity part can be described by relying on two common critical silica clusters, *i.e.* $(SiO_2)_{n1}$ and $(SiO_2)_{n2}$, which result from the self-polymerisation of silica. Consequently, the viscosity is calculated by Equation (6):

$$ln\,\eta = ln\,\eta_{ideal} + ln\,\eta_{excess} = \left(\sum_i x_i\, ln\,\eta_i\right) + (ln\,\eta_{SiO_2-pol.}) \quad (6)$$

where:
$\ln \eta_i = A_i + B_i/T$, $ln\,\eta_{SiO_2-pol.} = \sum_j (A_{(SiO_2)_{n_j}} + B_{(SiO_2)_{n_j}}/T) \cdot \left(x_{SiO_2}^{n_j}\right), j = 1,2$

η_{ideal} and η_{excess} are the ideal viscosity part and the excess viscosity part, respectively; X_i is the mole fraction of the monomeric associate species i; η_i is the viscosity contribution from the monomeric associate species i; $\eta_{SiO2-pol.}$ is the excess viscosity part resulting from the critical silica polymerisations; n_j is the integer coefficient that relates to a particular polymerisation degree; A_i and B_i are the temperature and composition independent constants respectively for the ideal viscosity part; $A_{(SiO2)nj}$ and $B_{(SiO2)nj}$ are the temperature and composition independent constants respectively for the excess viscosity part; T is the absolute temperature; and X^{nj}_{SiO2} is the weighting factor indicating the relative contribution of the excess viscosity part. The weighting factor is derived from the mole fraction of the critical silica cluster according to the chemical equilibrium between the monomeric associate species SiO_2 and the critical silica cluster $(SiO_2)_{nj}$:

$$x_{(SiO_2)_{n_j}} = K_{n_j} \cdot x_{SiO_2}^{n_j} \quad (7)$$

where $X_{(SiO2)nj}$ is the mole fraction of the critical silica cluster $(SiO_2)_{nj}$ and K_{nj} is an equilibrium constant for a particular degree of polymerisation. To simplify the equation, K_{nj} is implicitly incorporated into the model parameters $A_{(SiO2)nj}$ and $B_{(SiO2)nj}$. Moreover, a possible dependence of K_{nj} on temperature is ignored.

In the Al_2O_3-containing multicomponent systems, three kinds of Al^{3+}-containing associate species are employed to describe the Al^{3+}-induced structural change, *i.e.* non-tetrahedrons, Al^{3+}-based quasi-tetrahedrons, and Al^{3+}-based quasi-tetrahedrons bonded with SiO_2 tetrahedrons. These associate species indicate the different structural roles of Al^{3+} depending on composition and temperature and they are in dynamic equilibrium with each other.

For the type of non-tetrahedrons, *e.g.* in Al_2O_3, $Al_6Si_2O_{13}$, and $Na_2Al_4O_7$, Al^{3+} plays the role of a network modifier. When Al^{3+} is charge-compensated by Ca^{2+}, Mg^{2+}, Na^+ or K^+ and forms a quasi-tetrahedron, *e.g.* in $CaAl_2O_4$ and $NaAlO_2$, Al^{3+} behaves as a network former. Although these Al^{3+}-based quasi-tetrahedrons behave like a silica tetrahedron, these quasi-tetrahedrons themselves are not capable of forming large network structures. However, in case of quasi-tetrahedrons bonded with SiO_2 tetrahedrons, *e.g.* $NaSiAlO_4$ and $NaSi_3AlO_8$, large network structures can be formed by polymerisation.

To effectively describe the excess viscosity part for the Al_2O_3-containing multicomponent systems, two kinds of polymerisation are introduced, which are described as self- and inter-polymerisation. It is assumed that both the Al^{3+}-based quasi-tetrahedrons and silica tetrahedrons can self-polymerise. The self-polymerisation of silica is already described in Equation (6). A similar term is introduced to the excess viscosity part resulting from the self-polymerisation of the Al^{3+}-based quasi-tetrahedrons bonded with silica tetrahedrons. Besides the self-polymerisation, the Al^{3+}-based quasi-tetrahedrons can inter-polymerise with the silica tetrahedrons, which is considered by another excess viscosity part. Hence, the viscosity of the Al_2O_3-containing multicomponent systems is described with Equation (6), where the $\ln \eta_{excess}$ term is replaced by the following Equation (8):

$$\ln \eta_{excess} = \ln \eta_{self\text{-}pol.} + \ln \eta_{inter\text{-}pol.} \tag{8}$$

$$= \sum_j (A_{(SiO_2)_{n_j}} + B_{(SiO_2)_{n_j}}/T) \cdot \left(x_{SiO_2}^{n_j}\right) + \sum_k (A_{(Si-Al)_k} + B_{(Si-Al)_k}/T) \cdot \left(x_{(Si-Al)_k}^{n_k}\right) + \sum_m (A_{(Si-Al)_m} + B_{(Si-Al)_m}/T) \cdot \left(x_{(Si-Al)_m} \cdot x_{SiO_2}^{n_m}\right)$$

where j = 1,2; k = 1,2,3…; m = 1,2,3…; $(Si\text{-}Al)_k$ and $(Si\text{-}Al)_m$ are the silicon-aluminium based ternary associate species; n_k and n_m are the integer coefficient that relates to a particular degree of self-polymerisation and inter-polymerisation, respectively.

The capability of the model shall be demonstrated by two examples of challenging viscosity behaviour of oxide melts, namely the lubricant effect and the charge compensation effect. The so called lubricant effect, described by Avramov *et al.*[26], occurs in the SiO_2-based systems, in which the network modifiers, such as Al_2O_3, CaO, MgO, Na_2O and K_2O, play the role of lubricants allowing silica clusters to glide more easily with each other. Thus, the viscosity of molten silica decreases drastically when a small amount of network modifiers is added into the pure silica melt. In the current viscosity model, such structural change can be described by the monomeric associate species and two common critical silica clusters $(SiO_2)_6$ and $(SiO_2)_{109}$. As an example, Figure 5 shows the binary system SiO_2-Al_2O_3, which can be reproduced well for the temperature range 1800-2200°C.

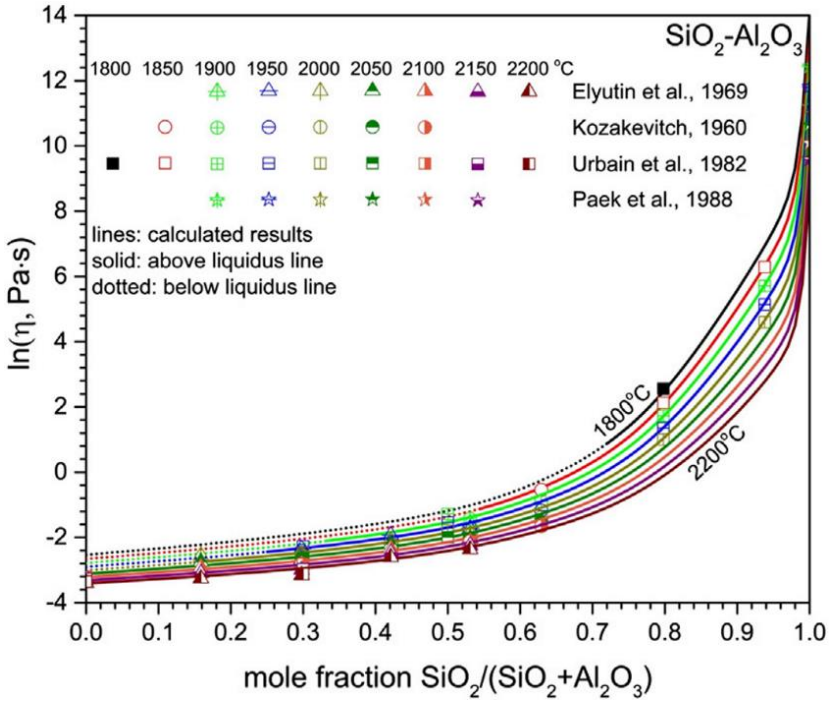

Figure 5: Comparison between experimental data and calculated data in the binary system SiO_2-Al_2O_3

The charge compensation or amphoteric effect, where amphoterics like Al_2O_3 and network modifiers like CaO, MgO, Na_2O and K_2O behave in combination as network formers, causes a local viscosity maximum as exemplarily shown in Figure 6 for the system SiO_2-Al_2O_3-Na_2O. This effect is naturally reflected by the calculations since the charge compensation species, in this system $NaAlO_2$, $NaSiAlO_4$ and $NaSi_3AlO_8$, are already associates that were chosen for the thermodynamic assessment.

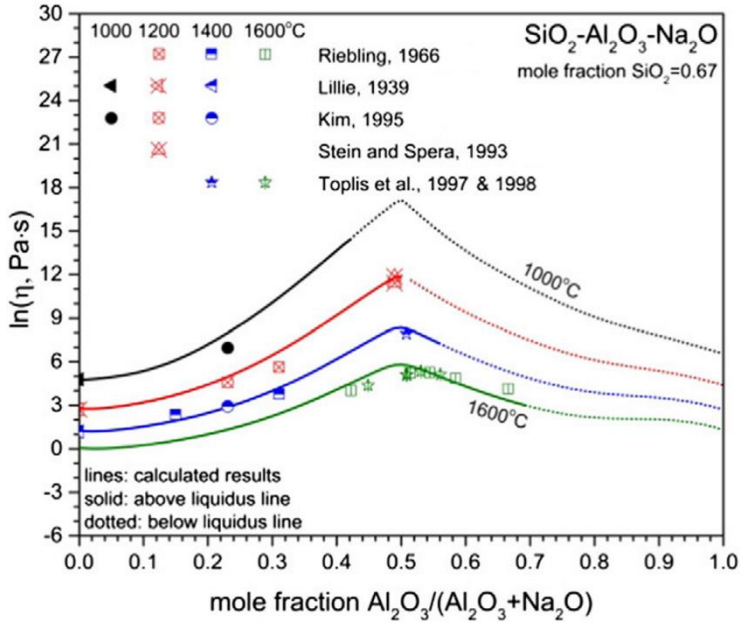

Figure 6: Comparison between experimental data and calculated data in the system SiO_2-Al_2O_3-Na_2O at 1000°C, 1200°C, 1400°C, 1600°C and 0.67 mole fraction SiO_2

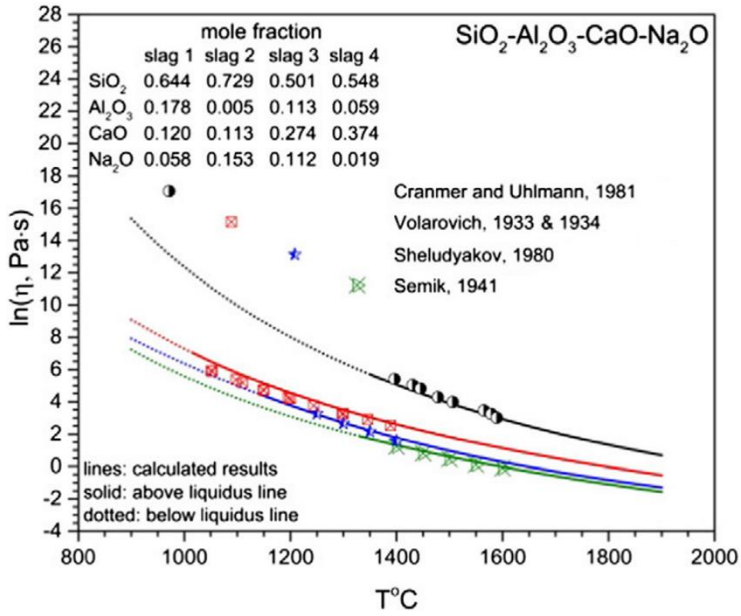

Figure 7: Comparison between experimental data and calculated data in the system SiO_2-Al_2O_3-CaO-Na_2O

For quaternary and higher order systems, the viscosity is extrapolated from the corresponding lower order systems without introducing additional associate species and additional model parameters. As an example, Figure 7 shows the dependence of the viscosity on temperature for several compositions in the system SiO_2-Al_2O_3-CaO-Na_2O. It is noted that the viscosities of the four slags follow the order slag 1 > slag 2 > slag 3 > slag 4, which is caused by the charge compensation effect. This order is

consistent with the order of the sum of the SiO_2 and Al_2O_3 contents although the amount of the charge compensators might not be enough for slag 1.

Influence of crystallisation

As illustrated in Figure 8, crystallisation has a physical as well as a chemical effect on the viscosity of a slag since it does not only transform the liquid into a dispersion but also changes the composition of the residual liquid, if it does not have a eutectic composition or is a pure oxide. The viscosity of the equilibrated partially crystallised slag η_{Eq} is calculated based on the viscosity of the super-cooled slag η_{Sc}. By thermodynamic equilibrium calculations the amount and composition of crystalline phases and remaining melt is calculated in dependence of temperature. Two factors are defined to describe the chemical and physical effect, respectively. The relative chemical viscosity $\eta_{r,chem}$ (Equation (9)) describes the effect caused by the change in chemical composition of the remaining melt (Rm) and the relative physical viscosity $\eta_{r,phys}$ (Equation (10)) the influence of particles. Thus, the viscosity of the partially crystallised melt under equilibrium can be calculated according to Equation (11). It shall be noted, that the change in chemical composition can either cause an increase of the viscosity, as shown in Figure 8, if the relative amount of network formers increases, or a decrease of the viscosity, if the relative amount of network modifiers increases.

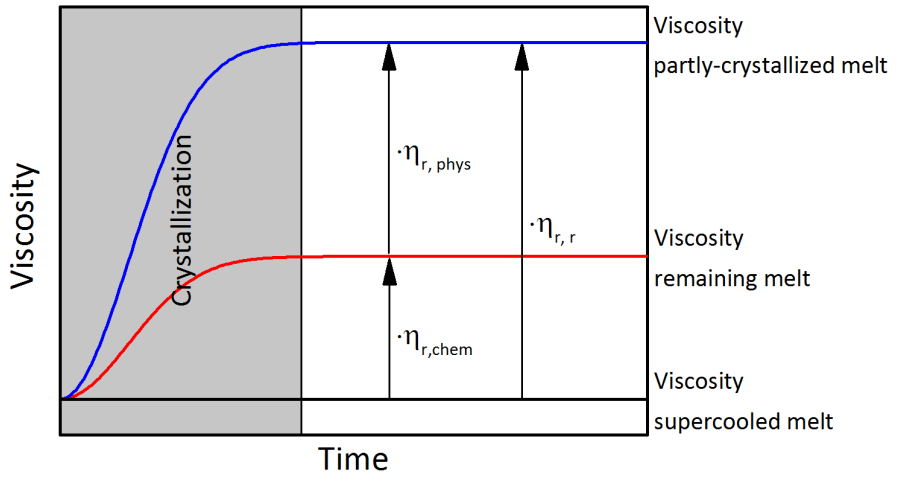

Figure 8: Concept of relative chemical and physical viscosity

$$\eta_{r,chem} = \eta_{Rm} / \eta_{Sc} \quad (9)$$

$$\eta_{r,phys} = \eta_{Eq} / \eta_{Rm} \quad (10)$$

$$\eta_{Eq} = \eta_{r,chem} * \eta_{r,phys} * \eta_{Sc} \quad (11)$$

The thermodynamic description can be extended by a kinetic description of the crystallisation process. Frequently the Kolmogorov-Avrami equation[27, 28] (Equation (12)) is used to describe the overall bulk isothermal crystallisation. As it uses

morphological information together with crystallisation mechanisms, it is capable of expressing the dependency of crystal volume with respect to time.

$$x(t) = 1 - \exp(-K*t^n) \quad (12)$$

In this equation x(t) is the degree of crystallisation at time t. The equation contains two parameters K and n, with n characterising the dimensional crystallisation growth.

The physical effect of particles depends on several parameters, *e.g.* volume, size and shape of particles. However, the volume fraction of the dispersed phase is the most crucial parameter. Einstein[29] developed one of the first theories for infinitely diluted solutions containing spherical particles. As seen from the Einstein Equation (Equation (13)) an increase of the volume of dispersed phase ϕ will lead to an increase of relative physical viscosity $\eta_{r,phys}$. Roscoe[30] extended the model to describe the flow of semi-concentrated dispersions. The so-called Einstein-Roscoe model (Equation (14)) is capable of describing the strong increase of relative viscosity by particle interactions at higher volume fractions of dispersed fluid. With further increasing crystalline volume non-Newtonian flow behaviour occurs. Since the mathematical nature of models derived from the Einstein-equation assumes Newtonian flow, power-law models like the Ostwald-de Waele[31] equations (Equation (15)) need to be consulted to describe the non-Newtonian flow of concentrated two-phase fluids depending on shear rate. In Equation (15) the consistency parameter K and the flow index n are necessary to describe the dependency of shear stress on strain rate of a non-Newtonian fluid. The flow index varies between shear-thinning (n < 1) and shear-thickening (n > 1). Depending on the volume fraction of dispersed phase derived from thermodynamic calculations, a suitable model for the calculation of the relative physical viscosity $\eta_{r,phys}$ needs to be selected.

$$\eta_{r,phys} = 1 + 2.5\phi \quad (13)$$

$$\eta_{r,phys} = (1 - b * \phi)^{-2.5} \quad (14)$$

$$\eta_{r,phys} = K * \dot{\gamma}^{n-1} \quad (15)$$

Conclusions

Besides temperature and composition, which determine the internal structure of an oxide melt, crystallisation in the slag significantly influences its flow behaviour. Therefore, not only the temperature dependent viscosity of fully liquid oxide slags was determined using a rotational high-temperature viscometer but also isothermal viscosity measurements were conducted, in order to examine the rheological evolution over time caused by the crystallisation. The crystallisation during flow can be separated into three time regimes: a lag time, in which the undercooled melt behaves as an Arrhenius-liquid; the kinetic-driven crystallisation; and finally, the

rheological equilibrium that is represented by a time-invariant viscosity plateau. To model the viscosity of oxide slags, in a first step a self-consistent thermodynamic database for multi-component oxide systems has been established. The Gibbs energy of the liquid phase has been modelled using a non-ideal associate solution description. In a second step, an Arrhenius-type model for the calculation of viscosities of fully molten slags has been developed. The model is based on the same structural units, *i.e.* the associates, as used for the Gibbs-energy model of the melt. In addition, by introduction of self- and interpolymerisation terms, the charge compensation effect and the lubricant effect (near pure SiO_2) can be described well with the new model. In a third step, the influence of crystallisation, which not only transforms the liquid into a dispersion but also usually changes the composition of the remaining liquid, on the viscosity is considered.

Acknowledgments

The work described in this paper has been performed in the framework of the projects HotVeGas, supported by the Federal Ministry for Economic Affairs and Energy (FKZ 0327773), and HVIGasTech, supported by the Helmholtz Association of German Research Centres (VH-VI-429).

References

1. C. Higman and M. van der Burgt, *Gasification*, Elsevier Science, Burlington, 2003.
2. M. Allibert ed., VDEh, *Slag atlas 1995*, Verlag Stahleisen, Dusseldorf, Germany, 1995.
3. S. Vargas, F. J. Frandsen and K. Dam-Johansen, "Rheological properties of high temperature melts of coal ashes and other silicates", *Prog Energy Combust Sci*, **27** (3) 237-429 (2001).
4. D. Tinker *et al.*, "High-pressure viscometry of polymerized silicate melts and limitations of the Eyring equation", *Am Mineral*, **89** (11-12) 1701-8 (2004).
5. W. H. Zachariasen, "The atomic arrangement in glass", *J Am Chem Soc*, **54** (10) 3841-51 (1932).
6. G. Urbain, Y. Bottinga and P. Richet, "Viscosity of liquid silica, silicates and aluminosilicates", *Geochim Cosmochim Acta*, **46** (6) 1061-72 (1982).
7. J. W. Nowok, J. P. Hurley and D. C. Stanley, "Local structure of a lignitic coal ash slag and its effect on viscosity", *Energ Fuels*, **7** (6) 1135-40 (1993).
8. A. Y. Ilyushechkin *et al.*, "The effect of solids and phase compositions on viscosity behaviour and TCV of slags from Australian bituminous coals", *J Non-Cryst Solids*, **357** (3) 893-902 (2011).
9. W. Song *et al.*, "Flow properties and rheology of slag from coal gasification", *Fuel*, **89** (7) 1709-15 (2010).
10. T. G. Mezger, *Das Rheologie Handbuch*, Vincentz, Hannover, Germany, 2012.
11. A. Kouchi, A. Tsuchiyama and I. Sunagawa, "Effect of stirring on crystallization kinetics of basalt: texture and element partitioning", *Contrib Miner Petrol*, **93** (4) 429-38 (1986).
12. S. Seebold, G. Wu and M. Müller, "The Influence of Crystallization on the Flow of Coal Ash-Slags", *Fuel*, **187** 376-87 (2017).
13. G. Wu, E. Yazhenskikh, K. Hack, E. Wosch and M. Müller, "Viscosity Model for Oxide Melts Relevant to Fuel Slags. Part 1: Pure Oxides and Binary Systems in the System SiO_2-Al_2O_3-CaO-MgO-Na_2O-K_2O", *Fuel Process Technol*, **137** 93-103 (2015).

14. G. Wu, E. Yazhenskikh, K. Hack and M. Müller, “Viscosity Model for Oxide Melts Relevant to Fuel Slags. Part 2: The System SiO2-Al2O3-CaO-MgO-Na2O-K2O”, *Fuel Process Technol*, **138** 520-33 (2015).
15. E. Yazhenskikh, K. Hack and M. Müller, “Critical thermodynamic evaluation of oxide systems relevant to fuel ashes and slags. Part 1: alkali oxide - silica systems”, *Calphad*, **30** 270-6 (2006).
16. E. Yazhenskikh, K. Hack and M. Müller, “Critical thermodynamic evaluation of oxide systems relevant to fuel ashes and slags. Part 2: alkali oxide - alumina systems”, *Calphad*, **30** 397-404 (2006).
17. E. Yazhenskikh, K. Hack and M. Müller, “Critical thermodynamic evaluation of oxide systems relevant to fuel ashes and slags. Part 3: silica - alumina systems”, *Calphad*, **32** 195-205 (2008).
18. E. Yazhenskikh, K. Hack and M. Müller, “Critical thermodynamic evaluation of oxide systems relevant to fuel ashes and slags. Part 4: sodium oxide - potassium oxide - silica”, *Calphad*, **32** 506-13 (2008).
19. E. Yazhenskikh, K. Hack and M. Müller, “Critical thermodynamic evaluation of oxide systems relevant to fuel ashes and slags, Part 5: Potassium oxide-alumina-silica”, *Calphad*, **35** 6-19 (2011).
20. E. Yazhenskikh, T. Jantzen, K. Hack and M. Müller, “Critical thermodynamic evaluation of oxide systems relevant to fuel ashes and slags: Potassium oxide - magnesium oxide - silica”, *Calphad*, **47** 35-49 (2014).
21. T. Jantzen, K. Hack, E. Yazhenskikh and M. Müller, “Evaluation of thermodynamic data and phase equilibria in the System Ca-Cr-Cu-Fe-Mg-Mn-S Part I: Binary and quasi-binary subsystems”, *Calphad*, (2016), http://dx.doi.org/10.1016/j.calphad.2016.04.011.
22. B. Sundman and J. Agren, “A regular solution model for phases with several components and sublattices, suitable for computer applications”, *J Phys Chem Solids*, **42** 297-301 (1981).
23. H. L. Lukas, S. Fries and B. Sundman, *Computational Thermodynamics: The Calphad Method*, Cambridge University Press, New York, USA, 2007.
24. T. M. Besmann and K. E. Spear, “Thermodynamic Modelling of Oxide Glasses”, *J Am Ceram Soc*, **85** 2887-2894 (2002).
25. J. O. M. Bockris, J. D. Mackenzie and J. A. Kitchener, “Viscous flow in silica and binary liquid silicates”, *Trans Faraday Soc*, **51** 1734-48 (1955).
26. I. Avramov, C. Rüssel and R. Keding, “Effect of chemical composition on viscosity of oxide glasses”, J *Non-Cryst Solids*, **324** 29-35 (2003).
27. A. N. Kolmogorov, “On the statistics of the crystallization process in metals”, *Bull Akad Sci USSR*, *Class Sci*, *Math Nat*, **1** 355-9 (1937).
28. M. Avrami, “Kinetics of phase change. II Transformation-time relations for random distribution of nuclei”, *J Chem Phys*, **8** (2) 212-24 (1940).
29. A. Einstein, “Berichtigung zu meiner Arbeit: Eine neue Bestimmung der Moleküldimensionen”, *Ann Phys*, **339** (3) 591-2 (1911).
30. R. Roscoe, “The viscosity of suspensions of rigid spheres”, *Br J Appl Phys*, **3** (8)267 (1952).
31. W. Ostwald and A. De Waele, “Oil and color”, *Chem Assoc J*, **6** 23-4 (1923).